Scilight

Photochemistry and Spectroscopy

https://www.sciltp.com/journals/ps

Supplementary Materials

Electron Bombardment of Amorphous Thione Ices—Thioacetamide as a Case Study

Sándor Góbi [1,*], Barbara Keresztes [1,2] and György Tarczay [1,3]

[1] Laboratory of Molecular Spectroscopy, Institute of Chemistry, ELTE Eötvös Loránd University, H-1518 Budapest, Hungary
[2] Hevesy György PhD School of Chemistry, Institute of Chemistry, ELTE Eötvös Loránd University, H-1518 Budapest, Hungary
[3] Centre for Astrophysics and Space Science, ELTE Eötvös Loránd University, H-1518 Budapest, Hungary
* Correspondence: sandor.gobi@ttk.elte.hu

How To Cite: Góbi, S.; Keresztes, B.; Tarczay, G. Electron Bombardment of Amorphous Thione Ices—Thioacetamide as a Case Study. *Photochemistry and Spectroscopy* **2025**, *1*(1), 3.

Table S1. Cartesian coordinates (Å) of ACN as optimized at the B3LYP/cc-pVTZ level of theory.

Atom	X	Y	Z
C	−0.144863	0.000020	−0.044182
N	−1.293787	−0.000097	−0.085742
C	1.309037	0.000151	0.008392
H	1.666512	0.886172	0.532034
H	1.666613	−0.884810	0.533755
H	1.721990	−0.000806	−0.999821

Table S2. Harmonic and anharmonic IR vibrational frequencies and intensities of ACN as computed at the B3LYP/cc-pVTZ level of theory.

Fundamental Bands Mode(Quanta)	E(harm)	E(anharm)	I(harm)	I(anharm)
1(1)	3115.402	2973.807	1.19825288	2.04892044
2(1)	3115.334	2975.283	1.19823162	2.07514997
3(1)	3047.817	2950.881	2.90263593	3.78532633
4(1)	2367.357	2337.312	9.67523766	9.25579241
5(1)	1475.433	1446.408	10.13795712	7.54224545
6(1)	1475.399	1446.419	10.13768216	7.54181284
7(1)	1414.436	1379.634	2.20508518	1.79686280
8(1)	1062.682	1041.677	2.08207042	2.24681561
9(1)	1062.656	1042.159	2.0813543	2.24352342
10(1)	928.048	922.034	1.23259587	1.03087607
11(1)	380.974	382.51	0.40117337	0.31795895
12(1)	380.932	383.102	0.40121855	0.31824658
Overtones Mode(Quanta)	E(harm)	E(anharm)		I(anharm)
1(2)	6230.804	5874.395		0.51866398
2(2)	6230.668	5899.892		0.52063101
3(2)	6095.635	5810.733		0.06414852
4(2)	4734.714	4643.305		0.01918153
5(2)	2950.866	2894.143		0.11560287
6(2)	2950.797	2854.732		0.11380309
7(2)	2828.872	2741.909		0.09662439
8(2)	2125.364	2077.752		0.08613620
9(2)	2125.313	2083.561		0.08632506
10(2)	1856.095	1834.942		0.04896011
11(2)	761.949	757.006		0.50307264
12(2)	761.864	768.956		0.51108918

Table S2. *Cont.*

Fundamental Bands Mode(Quanta)	**E(harm)**	**E(anharm)**	**I(harm)**	**I(anharm)**
Combination Bands Mode(Quanta)	E(harm)	E(anharm)		I(anharm)
2(1) 1(1)	6230.736	5911.883		0.28752411
3(1) 1(1)	6163.219	5823.525		0.20504183
3(1) 2(1)	6163.151	5825.454		0.20582128
4(1) 1(1)	5482.759	5305.918		0.02566623
4(1) 2(1)	5482.691	5307.396		0.0256789
4(1) 3(1)	5415.175	5254.257		0.00152345
5(1) 1(1)	4590.835	4401.939		0.2861909
5(1) 2(1)	4590.767	4412.027		0.30071563
5(1) 3(1)	4523.25	4349.07		0.12565441
5(1) 4(1)	3842.79	3778.158		0.00900861
6(1) 1(1)	4590.801	4410.477		0.30103419
6(1) 2(1)	4590.733	4403.101		0.28618875
6(1) 3(1)	4523.216	4349.135		0.12513021
6(1) 4(1)	3842.756	3778.169		0.00900968
6(1) 5(1)	2950.832	2889.769		0.00202888
7(1) 1(1)	4529.838	4344.442		0.36044385
7(1) 2(1)	4529.77	4346.169		0.36107083
7(1) 3(1)	4462.253	4312.848		0.03946487
7(1) 4(1)	3781.793	3710.700		0.07748612
7(1) 5(1)	2889.869	2821.193		0.11911380
7(1) 6(1)	2889.835	2821.283		0.11917566
8(1) 1(1)	4178.084	4007.142		0.05177735
8(1) 2(1)	4178.016	4012.156		0.04432424
8(1) 3(1)	4110.499	3958.728		0.16210961
8(1) 4(1)	3430.039	3372.086		0.00406819
8(1) 5(1)	2538.115	2487.365		0.06321767
8(1) 6(1)	2538.081	2487.368		0.20546165
8(1) 7(1)	2477.118	2416.580		0.22993882
9(1) 1(1)	4178.058	4010.805		0.04422118
9(1) 2(1)	4177.990	4009.504		0.05166332
9(1) 3(1)	4110.474	3959.337		0.16240064
9(1) 4(1)	3430.014	3372.57		0.00407216
9(1) 5(1)	2538.089	2487.828		0.20538338
9(1) 6(1)	2538.055	2487.999		0.06316815
9(1) 7(1)	2477.092	2417.244		0.23051816
9(1) 8(1)	2125.338	2086.488		0.02110990
10(1) 1(1)	4043.450	3898.126		0.00573154
10(1) 2(1)	4043.382	3899.608		0.00573182
10(1) 3(1)	3975.865	3845.264		0.01389983
10(1) 4(1)	3295.405	3253.842		1.00855750
10(1) 5(1)	2403.481	2367.858		0.00090013
10(1) 6(1)	2403.446	2367.869		0.00089990
10(1) 7(1)	2342.483	2292.055		0.32632535
11(1) 8(1)	1443.657	1419.575		2.30211056
11(1) 9(1)	1443.631	1420.107		1.54405155
11(1) 10(1)	1309.022	1310.514		0.00426606
12(1) 1(1)	3496.334	3356.769		0.00347967
12(1) 2(1)	3496.266	3359.111		0.08668175
12(1) 3(1)	3428.749	3305.647		0.00021875
12(1) 4(1)	2748.289	2710.863		0.24665687
12(1) 5(1)	1856.365	1833.788		0.13009725
12(1) 6(1)	1856.331	1834.364		0.00257152
12(1) 7(1)	1795.368	1761.798		0.00362422
12(1) 8(1)	1443.614	1420.181		1.54828127
12(1) 9(1)	1443.588	1420.879		2.29754928
12(1) 10(1)	1308.980	1311.118		0.00425384
12(1) 11(1)	761.906	774.197		0.00042220

Table S3. Summary of the CASINO simulations performed on the electron bombardment experiments.

	TA	TA–H_2O
Irradiated area (cm^2)	1.0 ± 0.1	1.0 ± 0.1
N[TA exposed] (10^{16} molecules cm^{-2})	5.1 ± 0.5	2.4 ± 0.2
Angle of incidence of electrons (°)	23	23
Irradiation time (s)	1800	1800
Nominal electron current (nA)	100	100
Initial energy of the electrons (keV)	5.00	5.00
Number of electrons generated (10^{15})	1.1 ± 0.1	1.1 ± 0.1
Average backscattered energy of electrons (keV)	3.2 ± 0.1	3.2 ± 0.1
Average transmitted energy of electrons (keV)	0.0 ± 0.0	0.0 ± 0.0
Fraction of backscattered electrons (%)	41 ± 3	41 ± 3
Fraction of transmitted electrons (%)	0.0 ± 0.0	0.0 ± 0.0
Simulated average penetration depth (nm)	80 ± 2	94 ± 3
Dose per TA molecule (eV)	16 ± 2	22 ± 4

Table S4. Infrared bands of neat amorphous TA ice.

Wavenumber (cm^{-1})		$I_{rel.}$ [b]	Assignment [c]
This Work [a]	Ref. [1]		
3281	3285	1.000	νas[NH2]
3164, 3101	3164, 3000	–	νs[NH2]
2962	2960	–	νas,i.p.[CH_3], νas,o.p.[CH_3]
2914	2910	–	νs[CH3]
1637	1638	0.048	β[NH_2]
1475	1472	0.030	(−)ν[CN] & βas,i.p.[CH3]
1431	1428	0.008	βas,o.p.[CH_3]
1397	1395	0.034	(+)ν[CN] & βas,i.p.[CH3]
1365	1366	0.013	βs[CH3]
1302	1300	0.028	ρ[NH_2]
1027	1026	0.004	ρ[CH_3]
972	970	0.019	ν[CC]
722	716	0.009	ν[CS]

[a] at 10 K after deposition; [b] Normalized experimental band areas. The values were obtained by dividing the integrated area of a band by the sum of the experimental band areas; [c] Assignments based on Ref. [1]. ν: stretching; β: bending; s: symmetric; as: antisymmetric; i.p.: in-plane; o.p.: out-of-plane; ρ: rocking vibrations; &: resonance between listed vibrational modes. The signs (−) and (+) denote in-phase and in-opposite-phase couplings between the coordinates that participate in the resonance.

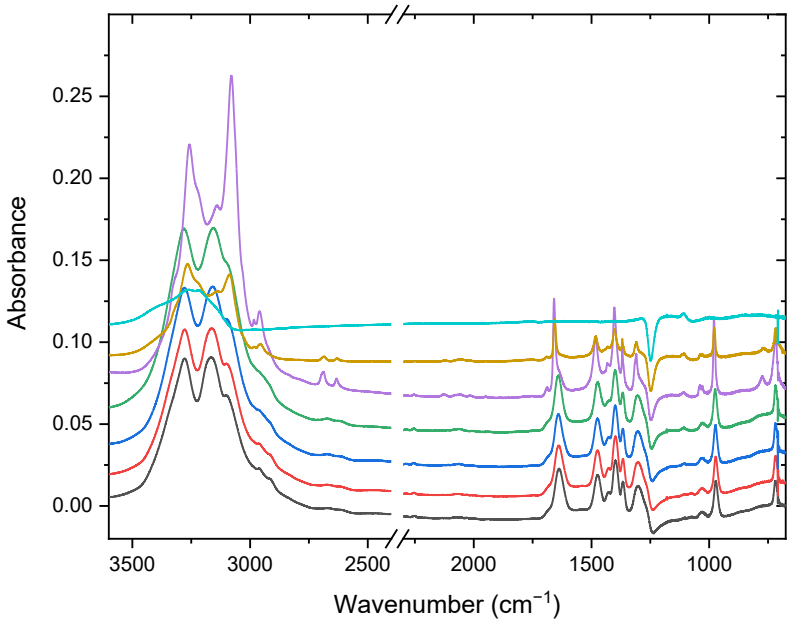

Figure S1. MIR spectra (3600–675 cm^{-1} region) of processed TA ice in the beginning of the TPD phase (black trace), at 50 K (red), 100 K (blue), 150 K (green), 200 K (purple), 250 K (dark yellow), and 300 K (turquoise), respectively. The spectra are offset for clarity.

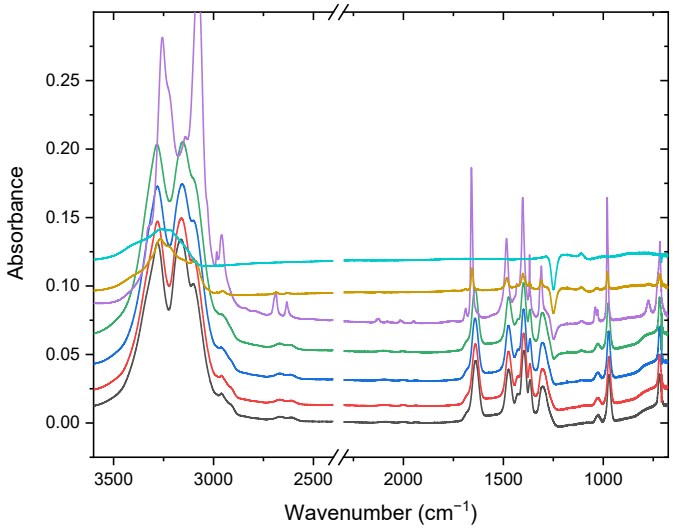

Figure S2. MIR spectra (3600–675 cm^{-1} region) of neat TA ice (blank experiment) in the beginning of the TPD phase (black trace), at 50 K (red), 100 K (blue), 150 K (green), 200 K (purple), 250 K (dark yellow), and 300 K (turquoise), respectively. The spectra are offset for clarity.

Table S5. Infrared bands of the amorphous TA–H_2O ice mixture.

Wavenumber (cm^{-1})		$I_{rel.}$ [b]	Assignment [c]
This Work [a]	Ref. [1]		
3304	3285	1.000	vas[NH2]
1651	1638	0.058	β[NH_2]
1485	1472	0.030	(−)ν[CN] & βas,i.p.[CH3]
1430	1428	0.007	βas,o.p.[CH_3]
1405	1395	0.025	(+)ν[CN] & βas,i.p.[CH3]
1372	1366	0.010	βs[CH3]
1310	1300	0.022	ρ[NH_2]
1042	1026	0.005	ρ[CH_3]
972	970	0.014	ν[CC]
718	716	0.006	ν[CS]

[a] at 10 K after deposition; [b] Normalized experimental band areas. The values were obtained by dividing the integrated area of a band by the sum of the experimental band areas. The H_2O bands were compensated for. [c] Assignments based on Ref. [1]. ν: stretching; β: bending; s: symmetric; as: antisymmetric; i.p.: in-plane; o.p.: out-of-plane; ρ: rocking vibrations; &: resonance between listed vibrational modes. The signs (−) and (+) denote in-phase and in-opposite-phase couplings between the coordinates that participate in the resonance.

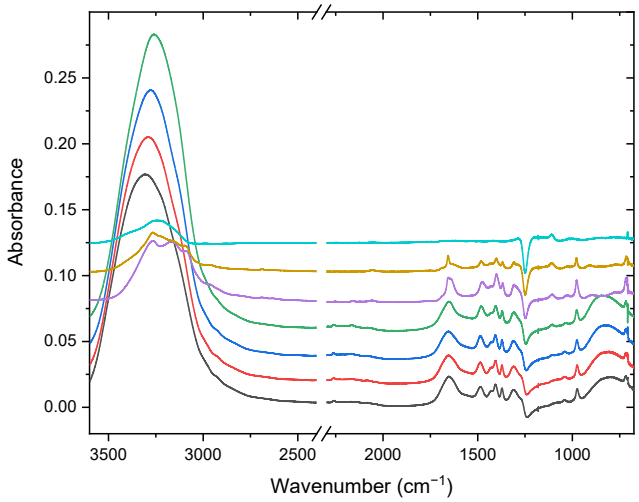

Figure S3. MIR spectra (3600–675 cm^{-1} region) of processed TA–H_2O ice mixture in the beginning of the TPD phase (black trace), at 50 K (red), 100 K (blue), 150 K (green), 200 K (purple), 250 K (dark yellow), and 300 K (turquoise), respectively. The spectra are offset for clarity.

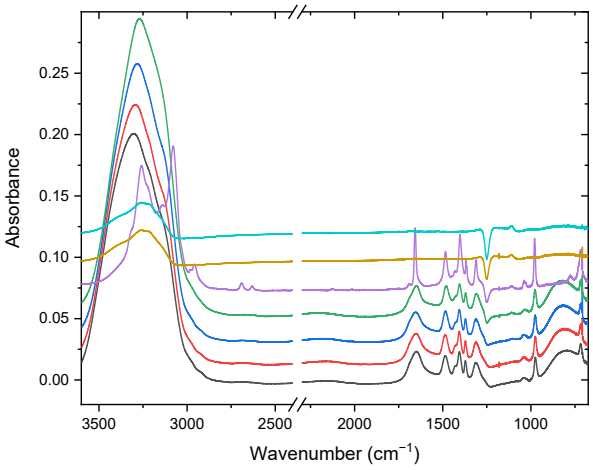

Figure S4. MIR spectra (3600–675 cm^{-1} region) of the neat TA–H_2O ice mixture (blank experiment) in the beginning of the TPD phase (black trace), at 50 K (red), 100 K (blue), 150 K (green), 200 K (purple), 250 K (dark yellow), and 300 K (turquoise), respectively. The spectra are offset for clarity.

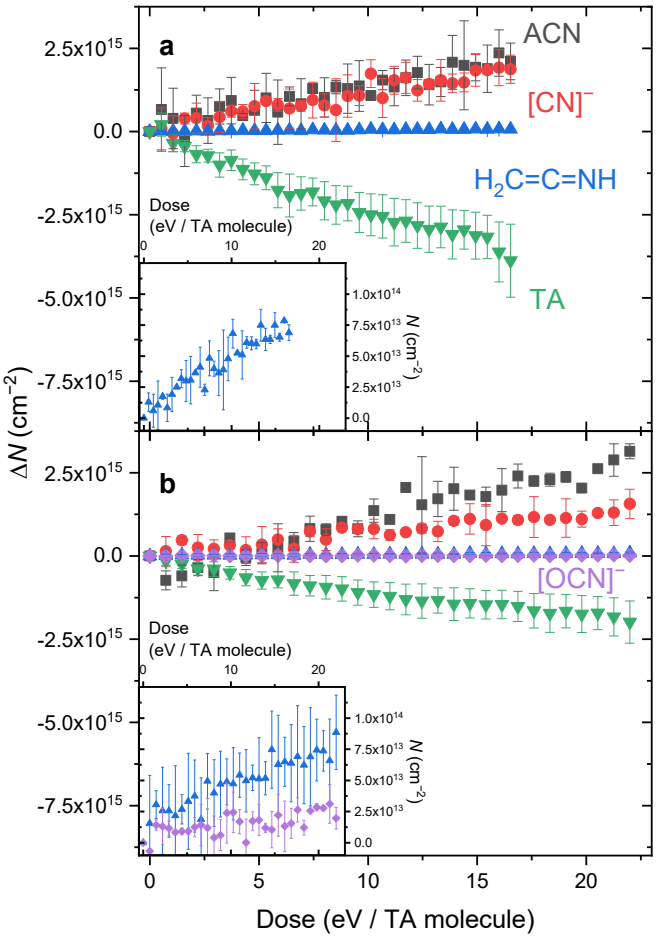

Figure S5. Change of *N* of TA (green upside-down triangles) as well as the products ACN (black squares), $[CN]^-$ (red circles), and $H_2C=C=NH$ (blue triangles) during the fourth electron bombardment cycle of (**a**) the neat amorphous TA experiment; (**b**) the TA–H_2O experiment (full version). The insets show blowups of the figures for $H_2C=C=NH$ and $[OCN]^-$.

References

1. Góbi, S.; Reva, I.; Tarczay, G.; et al. Amorphous and crystalline thioacetamide ice: Infrared spectra as a probe for temperature and structure. *J. Mol. Struct.* **2020**, *1220*, 128719.